

Nearest-neighbor Ising model with a uniaxial incommensurate phase and a Lifshitz point

Eytan Domany and Bernd Schaub

Department of Electronics, Weizmann Institute of Science, Rehovot 76100, Israel

(Received 26 August 1983)

The anisotropic triangular nearest-neighbor Ising model, with antiferromagnetic interactions, is studied. The phase diagram, as a function of temperature and field, has a complex structure. Two commensurate ordered phases are found. The transition to one is Ising-type. The second is reached from the disordered phase in one of two ways: either via an intermediate uniaxial incommensurate phase—which is reached at high temperatures by a Kosterlitz-Thouless transition and at low temperatures undergoes an incommensurate-commensurate transition—or by a single continuous transition. The latter transition is in the same universality class as the chiral three-state Potts model, with thermal exponent within 4% of that of the three-state Potts model. These two transition regimes are found to be separated by a Lifshitz point. The phase diagram and critical behavior were determined by analytical (symmetry analysis and free-fermion approximation) as well as numerical (phenomenological renormalization-group and Monte Carlo) methods.

I. INTRODUCTION

Considerable progress was made in recent years in our theoretical understanding of the phase structure and nature of transitions in a variety of two-dimensional models. Some of the most recent, important developments range from rigorous solutions,¹⁻³ through analytic results (believed to be exact),⁴ establishment of connections between the critical manifold of various models and the Gaussian model,⁵ to development of powerful numerical approximation schemes.^{6,7}

In parallel, dramatic progress in experimental techniques allowed detailed comparison of theory and experiments^{8,9} (especially on adsorbed monolayers). Connections between theoretical models and physical systems were established on the basis of symmetry arguments.¹⁰

In this paper, we present detailed investigations of a particularly simple two-dimensional model, which has a complex and rich phase structure.¹¹ By studying this model, one hopes to resolve some important open questions of critical phenomena in two dimensions.

A class of models that was extensively studied has competing ground states (as some parameter is varied). Such is the case for the anisotropic next-nearest-neighbor Ising (ANNNI) model,¹²⁻¹⁴ the chiral Potts (CP) model,^{15,16} and a lattice-gas model (H/Fe), describing adsorption of H on Fe(110).¹⁷ In all three cases, the transition temperature vanishes at a special degeneracy point; all three exhibit incommensurate phases (and, therefore, commensurate-incommensurate transitions) and, possibly, Lifshitz points.¹⁸ We believe that the model we consider exhibits these features and is simpler (in terms of the interactions and/or the basic variable) than the models mentioned above. First, we mention briefly some of the theoretical problems one may hope to resolve by extensive studies of our model.

The first problem, as posed originally by Ostlund,^{15,19}

can be stated in terms of the CP model. For vanishing chirality, the critical behavior is determined by the three-state Potts fixed point. If chirality is introduced, one may ask whether the respective operator is relevant or irrelevant. If relevant, does the system cross over to a new fixed point with different exponents? Will there be a line of transition points, separating the disordered and ordered phases, controlled by such a new fixed point?

Even though the chiral operator was found to be relevant, a most recent calculation by den Nijs²⁰ gave the value $\frac{1}{6}$ for the crossover—it is by no means clear that the new stable fixed point is characterized by different exponents.

Alternatively, the question can be phrased in terms of the symmetry arguments that were widely used to identify the universality classes of various transitions.¹⁰ Almost all classification schemes were restricted to cases for which the Lifshitz condition is satisfied. This condition states that the ordered state is characterized by a Fourier expansion with wave vector \vec{k}_0 , such that the coefficient of the second-order (in the order parameter) term in the Landau-Ginzburg (LG) free energy has a minimum (as a function of \vec{k}) at \vec{k}_0 . That is, terms linear in $\vec{k} - \vec{k}_0$, and quadratic in the order parameter are ruled out on the basis of symmetry. When this condition is not satisfied, mean-field theory allows a continuous transition only if the \vec{k} vector varies continuously in the ordered phase, i.e., it is incommensurate.²¹ If the transition is to a state with commensurate \vec{k}_0 , for which the Lifshitz condition is not satisfied, mean-field theory implies that \vec{k}_0 is stabilized by a term *higher than quadratic* in the order parameter, and therefore the transition must be first order.

If this statement were correct in two dimensions, it would imply that transitions from disordered to (a) the commensurate phases of the CP model,¹⁵ (b) the $\langle 2 \rangle$ phase of the ANNNI model,¹²⁻¹⁴ as well as (c) the 3×1 phase of the H/Fe model¹⁷ must either occur via an intermediate incommensurate phase, or be first order.

However, the prediction that a transition, if governed by third- or higher-order terms in the LG Hamiltonian, *must* be first order, is based on mean-field theory, and is known to be violated in two dimensions. Thus one would expect that a single, continuous transition would be possible. This raises two questions. The *first* concerns the relevance of the Lifshitz (or chiral) term, and the fixed point to which the system crosses over, as stated above.

A *second* question concerns the manner in which the transition from disordered to commensurate state changes its nature; if for some values of a parameter $p < p_c$ it proceeds via an intermediate incommensurate phase, and for $p > p_c$ a single continuous transition occurs, one may have^{13,16,19,22,23} a Lifshitz point at $p = p_c$, whose properties in two dimensions are not yet known.

In the case of the ANNNI model, evidence for a Lifshitz point has been found,¹³ but statements to the contrary have also been made. In the case of the CP model, existence of a Lifshitz point was suggested¹⁵ and its location estimated using different numerical methods.^{16,23} However, recent analytical calculations,²⁴ done in the limit of vanishing dislocation density, indicate the absence of a Lifshitz point. If such is the case, the transition from disordered to commensurate phase must proceed via an intermediate floating phase, except at an isolated point of three-state Potts character.

In either case, such a floating phase is predicted to be reached from the disordered phase via a Kosterlitz-Thouless transition.²⁵ As the temperature is lowered, a commensurate-incommensurate transition about whose properties a variety of predictions have recently been given,^{26–28} will occur. Thus one may hope to confirm, by studying our model, the predictions concerning both the disordered-incommensurate and incommensurate-commensurate transitions.

The techniques used in this work are symmetry analysis,¹⁰ free-fermion approximation,¹⁴ the phenomenological renormalization-group method,⁷ and Monte Carlo simulation. Symmetry analysis confirms that at one of the commensurate phases the Lifshitz condition is not satisfied. Disregarding the Lifshitz term leads to the LG Hamiltonian of the three-state Potts model. Thus we establish the connection to the CP and H/Fe models.

The free-fermion approximation (exact at low temperatures near the degeneracy point) establishes the existence of a floating phase.¹⁴ The phenomenological renormalization-group (transfer-matrix) method yields a phase diagram, identifies regions where evidence for a floating phase are found, indicates the existence of a Lifshitz point, and provides estimates for critical exponents. Finally, Monte Carlo simulations are used to calculate specific-heat curves. Also, by calculating how the susceptibility and $\chi(q)$ scale with size,²⁹ further evidence for the floating phase and the existence of a Lifshitz point is obtained.

The model is introduced in Sec. II, which also contains the symmetry analysis. The free-fermion approximation is presented in Sec. III. Phenomenological renormalization-group results and Monte Carlo simulations are discussed in Secs. IV and V, respectively. In Sec. VI our findings are summarized and discussed.

II. THE MODEL AND ITS SYMMETRY

We consider the antiferromagnetic Ising model on an anisotropic triangular lattice in an external field [anisotropic triangular nearest-neighbor Ising (ATNNI) model]. By uniaxial distortion, the triangular lattice becomes centered rectangular [see Fig. 1(a)]; such a lattice of adsorption sites is provided by the (110) face of a bcc crystal. The Hamiltonian can be written as ($S_i = \pm 1$)

$$\mathcal{H} = J \sum_i \left[\sum_{\hat{\delta}=\hat{1},\hat{2}} S_i S_{i+\hat{\delta}} + \alpha S_i S_{i+\hat{3}} - (H/J) S_i \right], \quad (2.1)$$

with $J > 0$, $0 < \alpha < 1$, and the directions $\hat{1}, \hat{2}, \hat{3}$ as indicated in Fig. 1(a).

The partition sum is given by

$$Z = \sum_{\{S\}} \exp[-\mathcal{H}/T], \quad (2.2)$$

and we use the normalization $J = 1$, with H/J denoting the (dimensionless) ratio of the field and the nearest-neighbor coupling, and T/J denoting the (dimensionless) temperature. For $H = 0$, the model is exactly soluble,³⁰ and has a transition given by $\cosh(4J/T_c) = \exp(4\alpha J/T_c)$ ($T_c/J \approx 1.55$ for $\alpha = 0.4$). For $H \neq 0$, Verhagen³¹ has solved the model on a special (disorder) line, given by

$$\sinh^2 \left[\frac{H}{T} \right] = \frac{\exp(-4\alpha J/T) \cosh^2(2J/T) - 1}{\exp(-4J/T) \exp(4\alpha J/T) - 1}. \quad (2.3)$$

On this line the model has no transition; it lies entirely in the disordered phase. For $T \rightarrow 0$, one obtains from (2.3)

$$H/J = (H/J)^* = 4(1 - \alpha). \quad (2.4)$$

Lin and Wu³² noted recently that precisely at this value of H/J the ground state changes. For $H/J < (H/J)^*$ the

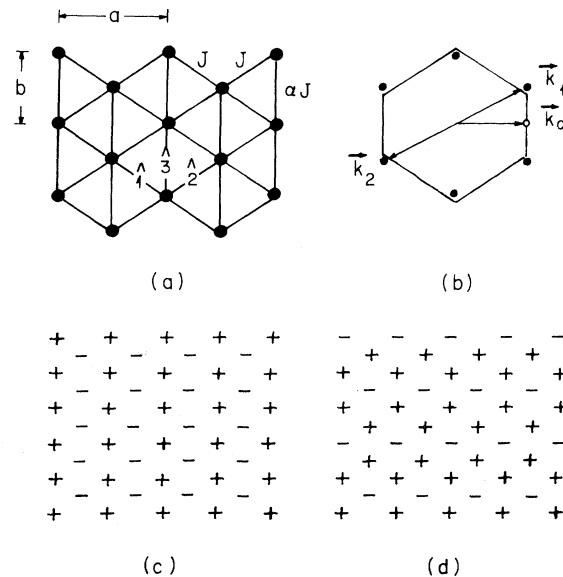


FIG. 1. (a) Centered rectangular lattice. Along directions $\hat{1}$ and $\hat{2}$ the interaction is J ; along $\hat{3}$ it is αJ . (b) First Brillouin zone. (c) \vec{k}_0 characterizes structure I; (d) \vec{k}_1 and \vec{k}_2 characterize structure II. Note that \vec{k}_1 and \vec{k}_2 are *not* at the zone corners.

ground state is the 2×1 structure I of Fig. 1(c), while for $(H/J)^* < H/J < 2(2+\alpha)$ it is the structure II of Fig. 1(d). Note that for a triangular lattice, II is the $\sqrt{3} \times \sqrt{3}$ structure. For $H/J > 2(2+\alpha)$, the ground state is $S_i = +1$. Lin and Wu calculated the boundary of phase I by the interface method³³ and proposed a schematic phase diagram in the entire H, T plane [Fig. 2(a)]. Subsequently, Doczi-Reger and Hemmer³⁴ extended the work of Lin and Wu. They noted that at the special value $(H/J)^*$ the ground state is highly degenerate, which drives the transition temperature to zero; they also calculated the boundary of phase II by the interface method and proposed the phase diagram of Fig. 2(b). Our phase diagram is presented in Fig. 2. Thus the present model, with Ising variables (as opposed to the three states of the CP model) and nearest-neighbor interactions only (as opposed to the ANNNI and H/Fe models) exhibits all the interesting features mentioned in Sec. I; it has competing ground states, a disorder line, and disordered phase extending to $T=0$. We find a floating phase, a commensurate-incommensurate transition, and a Lifshitz point, beyond which phase II is reached in a single transition of CP character (see below).

Additional exact information is provided by the hard hexagon model.¹ Near the point $H/J = 2(2+\alpha)$ the model reduces³⁵ to the hard hexagon model whose critical fugacity Z_c determines the exact slope of the phase boundary as³⁵

$$\begin{aligned} T_c/J &= (1/a)[(H/J)_c - 2(2+\alpha)], \\ a &= -\frac{1}{2} \ln Z_c = -\frac{1}{2} \ln \left[\frac{1}{2} (11 + 5\sqrt{5}) \right] \simeq -1.20, \end{aligned} \quad (2.5)$$

thus the nature of the transition at the upper degeneracy

point is expected to be three-state Potts. We now turn to analyze the symmetry of the model, and construct the LG Hamiltonian associated with its transitions.

The symmetry group is $C2mm$. The lattice and the first Brillouin zone are shown in Figs. 1(a) and 1(b). At the reciprocal-lattice vector $\vec{k}_0 = (2\pi/a, 0)$ the Lifshitz condition is satisfied; $\exp(i\vec{k}_0 \cdot \vec{r})$ belongs to a one-dimensional representation, gives rise to the structure I of Fig. 1(c), and the transition to this structure is in the Ising universality class.¹⁰ The structure of II of Fig. 1(d) belongs to a two-dimensional representation; of the six reciprocal-lattice vectors [denoted by closed circles in Fig. 1(b)] only two are independent. Note that the closed circles are *not* at the zone corners.

One may choose $\vec{k}_{1,2} = \pm(2\pi/a, 2\pi/3b)$ as the star that spans a two-dimensional representation. At these wave vectors the Lifshitz condition is not satisfied; therefore, mean-field theory would predict a continuous transition to an incommensurate structure characterized by wave vectors $\pm \vec{k} = (2\pi/a, 2\pi q/3b)$ with $0 < q < 1$. The LG Hamiltonian for the transition to such a state contains only terms of the form $(\psi_{\vec{k}} \psi_{-\vec{k}})^n$, and therefore an xy -type transition is expected.²⁵ However, for the commensurate ($q=1$) case, a third-order invariant of the form $\psi_{\vec{k}}^3 + \psi_{-\vec{k}}^3$ is allowed, and disregarding the Lifshitz term (and higher-order \vec{k} -dependent invariants) one obtains the LG Hamiltonian of the three-state Potts model.^{36,10}

Thus mean-field theory would predict either a continuous transition to an incommensurate structure, followed by an incommensurate-commensurate transition at which the \vec{k} vector "locks in" at the value $\pm \vec{k}_1$, or a direct,

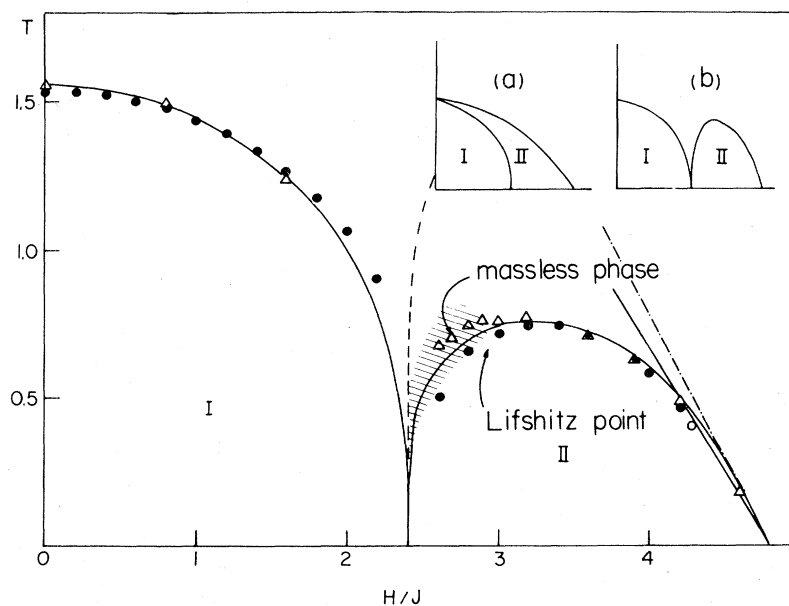


FIG. 2. Phase diagram for the ATNNI model (2.1) with $\alpha=0.4$. Closed circles—using Eq. (4.4) with strips of widths 8,10. Triangles, specific-heat maxima from Monte Carlo on 24×24 systems. Dashed lines, low-temperature boundary separating phase II from the incommensurate phase [Eq. (3.13)]; solid line, boundaries determined by the interface method. Indications for incommensurate phase were found in the shaded region. Solid and dotted-dashed lines near $H/J = 4.8$ have the asymptotic slope as determined from the hard hexagon model and the interface method, respectively. Schematic phase diagrams, as obtained in (a) Ref. 32 and (b) Ref. 34.

first-order transition to structure II. This latter transition could be continuous in two dimensions. In the mean-field description, this transition is dominated by the third-order (umklapp) terms, and the fact that the minimum of the term quadratic in the order parameter is *not* at \vec{k}_1 plays no role whatsoever. If fluctuations (known to be important in two dimensions) do not alter this picture, and the transition is still governed by the third-order terms, one would expect the single transition to be in the three-state Potts universality class, in spite of the Lifshitz term. Even if the latter is relevant (in the renormalization-group sense) as shown by den Nijs,²⁰ the system could still exhibit critical behavior which is also three-state Potts-type [as is the case for an Ising antiferromagnet in a (relevant) uniform field, which exhibits Ising-to-Ising crossover, and the liquid-gas transition with the (redundant) ϕ^3 operator]. The questions, whether the ATNNI model does or does not have both kinds of behavior (intermediate floating phase *and* a direct transition) and if so, what is the nature of the direct transition, where is the Lifshitz point, etc., can possibly be resolved only through detailed numerical investigations.

III. FREE-FERMION APPROXIMATION

Recently, Villain and Bak¹⁴ analyzed the ANNNI model near its degeneracy point using a free-fermion approximation. They have shown that a region of incommensurate phase exists near the boundary of the $\langle 2 \rangle$ phase. In this section we adapt their method to treat the ATNNI model.

For $H/J = 4(1-\alpha) = (H/J)^*$ the ground state of the ATNNI model is highly degenerate, whereas for $H/J < 4(1-\alpha)$ the ground state is doubly degenerate. The configuration I of Fig. 1(c) has the same energy as the configuration I' obtained from I by reversing all spins. The degeneracy at $(H/J)^*$ is caused by competition between the interactions and the external field. The interactions cause an energetic cost for any interface I/I' of $\Delta E^{int} = 4N_x J(1-\alpha)$ (see Fig. 3 for definition of N_x). This cost can be compensated only by lowering of the energy due to the external field. This is possible only if the interface creates a region with a high density of + spins, which are preferred by the field, as is shown in Fig. 3. So one can identify two kinds of interfaces. To set up notation, we assign integer-valued coordinates (n_x, n_y) to the sites of + spins in I, and half-integer $(n_x + \frac{1}{2}, n_y + \frac{1}{2})$ to sites with -. A *wall* separates I (for small n_y) from I' (for large n_y) and passes between n_y and $n_y + \frac{1}{2}$; an *antiwall* separates I' (for small n_y) from I (for large n_y) and passes between $n_y - \frac{1}{2}$ and n_y . At the degeneracy point $(H/J)^*$, all structures of any alternating wall-antiwall sequence are degenerate with I and I'; the energetic cost per one smooth wall (or antiwall) is

$$E_w = N_x J [(H/J)^* - H/J] . \tag{3.1}$$

In order to study the statistical mechanics of interfaces near the degeneracy point $(H/J)^*$ and for $T \simeq 0$, we characterize the position of a smooth wall or antiwall by

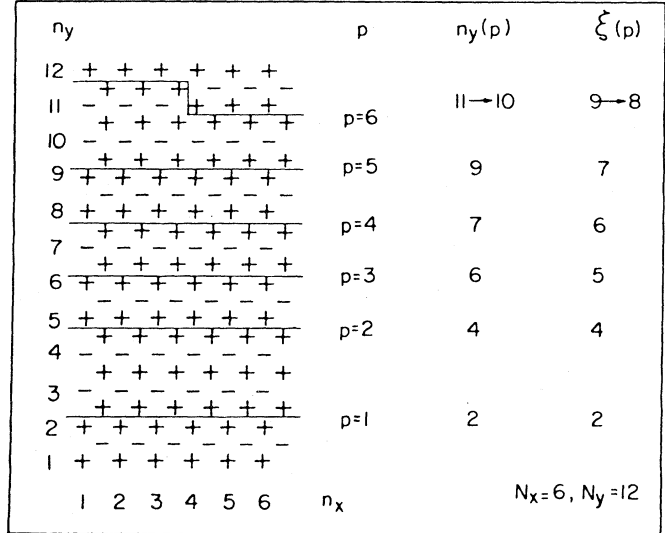


FIG. 3. Notation used in the free-fermion approximation. A lattice with $N_x=6$ and $N_y=12$, with $p=1,2, \dots, 6$ interfaces, characterized by $n_y(p)$ and the reduced wall coordinate $\xi(p)$. Densest packing of walls ($2 \leq p \leq 5$) yields phase II; $p=6$ wall has a single-step excitation.

the integer coordinate above which it passes. The interfaces of a configuration of ν alternating walls and antiwalls can be sequentially numbered by indices $p=1,2, \dots, \nu$, such that for odd p we have a wall, for even p an antiwall with $n_y(p) > n_y(p-1)$. Besides we must have

$$n_y(2p+1) - n_y(2p) \geq 2, \quad n_y(2p) - n_y(2p-1) \geq 1 . \tag{3.2}$$

The densest possible wall-antiwall sequence yields structure II which can be seen by comparing the region $5 \leq n_y \leq 9$ in Fig. 3 with Fig. 1(d). In this case the wall density is $\bar{q} = \nu/N_y = \frac{2}{3}$. We can define a reduced interface coordinate

$$\xi_p = N_y(p) = - \left\lfloor \frac{p-1}{2} \right\rfloor \tag{3.3}$$

(the square brackets denote integer part) in terms of which the restrictions (3.2) take the form

$$\xi_{p+1} - \xi_p \geq 1 . \tag{3.4}$$

In order to study the excitations of a smooth interface, we will consider single-step changes of $n_y(p) \rightarrow n_y(p) \pm 1$ whose energetic cost is $4J$ (for $\alpha < 0.5$). These single-step changes are the dominant excitations at low temperatures. By using the Villain-Bak formalism,¹⁴ the partition sum $Z(\nu)$ corresponding to ν interfaces is given by

$$Z(\nu) = E_0^{N_x} \exp(-\beta \nu E_w) C(\nu) , \tag{3.5}$$

where E_w is given by (3.1), $C(\nu)$ reflects boundary effects that can be neglected in the thermodynamic limit, and E_0 is the largest eigenvalue of the transfer matrix $e^{-\beta \mathcal{H}}$ with \mathcal{H} a free-fermion Hamiltonian

$$\hat{\mathcal{H}} = -2\gamma \sum_k C_k^\dagger C_k \cos k, \quad (3.6)$$

where $\gamma = e^{-4\beta J}$ denotes the Boltzmann weight associated with a single-wall excitation.

The ground state of (3.6) is

$$|0\rangle = \prod_{-k_f < k < k_f} C_k^\dagger |vac\rangle, \quad (3.7)$$

which gives

$$E_0(\nu) = \exp \left[2\gamma \sum_{k=-k_f}^{k_f} \cos k \right]. \quad (3.8)$$

Since the largest value that ξ_ν can take is

$$\xi_\nu(\max) = N_y - \left\lfloor \frac{\nu-1}{2} \right\rfloor \approx N_y - \nu/2,$$

the spacing in k space is $\Delta k = 2\pi/(N_y - \nu/2)$ which leads to

$$k_f = \pi\nu(N_y - \nu/2) \quad (3.9)$$

(using $\nu = 2k_f/\Delta k$). So finally, we obtain

$$E_0(\nu) = \exp \left[\frac{2\gamma}{\pi} (N_y - \nu/2) \sin \left[\frac{\pi\nu}{N_y - \nu/2} \right] \right]. \quad (3.10)$$

Now the expression for $Z(\tilde{q})$, where $\tilde{q} = \nu/N_y$ is the interface density, has to be minimized with respect to \tilde{q} ,

$$Z(\tilde{q}) = \exp \left[2\gamma N_x N_y \left[\frac{1-\tilde{q}/2}{\pi} \sin \frac{\pi\tilde{q}}{1-\tilde{q}/2} - \tilde{q}A \right] \right], \quad (3.11)$$

where

$$A = \frac{\beta J}{2\gamma} [(H/J)^* - H/J], \quad (3.12)$$

minimizing (3.11), yields three distinct regions as follows:

- (1) $(H/J)^* - H/J \geq 2e^{-4\beta J}/\beta J$,
- (2) $H/J - (H/J)^* \geq 3e^{-4\beta J}/\beta J$,
- (3) $-2e^{-4\beta J}/\beta J < H/J - (H/J)^* < 3e^{-4\beta J}/\beta J$.

In regions (1) and (2), the commensurate phases I ($\tilde{q}=0$, i.e., no walls) and II ($\tilde{q}=\frac{2}{3}$, i.e., densest-wall configuration) are stable against interface formation. In region (3) an incommensurate phase appears, in which \tilde{q} varies smoothly between 0 and $\frac{2}{3}$ and is given by the solution of

$$\frac{1}{2\pi} \sin \left[\frac{\pi\tilde{q}}{1-\tilde{q}/2} \right] + \frac{1}{1-\tilde{q}/2} \cos \left[\frac{\pi\tilde{q}}{1-\tilde{q}/2} \right] - A = 0. \quad (3.14)$$

Incorporation of vortices will lead to instability of this phase with respect to the high-temperature paramagnetic phase. This instability is expected^{14,37} near phase I, leaving a narrow strip of stable incommensurate phase near the boundary of phase II, as indicated in Fig. 2. However,

whether this region ends at a finite-temperature Lifshitz point or not cannot be resolved by this analysis which is based on an expansion near the $T=0$ degeneracy point. Therefore, we addressed this question by two numerical methods: a phenomenological renormalization-group method and Monte Carlo simulation.

IV. PHENOMENOLOGICAL RENORMALIZATION GROUP

This numerical technique is based on diagonalization of the row-to-row transfer matrix for an infinite strip of finite width. Nightingale, who used this procedure in conjunction with finite-size scaling, has called the resulting method "phenomenological renormalization group."⁷

The technique has since been extensively used and shown to provide one of the most reliable methods to determine phase boundaries and critical exponents, as well as to establish the existence of massless phases.⁷ By iterative diagonalization we determine the largest three eigenvalues $\lambda_0 > |\lambda_1| \geq |\lambda_2|$ of the transfer matrix T associated with the lattice of Fig. 4. We chose the value $\alpha=0.4$ for numerical investigation of model (1). Throughout this section we denote by H/J the ratio of the field to the large nearest-neighbor coupling, and by J we denote the inverse temperature.

For our model (2.1) we chose strips as depicted in Fig. 4, with a periodic boundary condition. In order to accommodate both ground states I and II of Fig. 1, we were restricted to work with strips of even width. It is important to note that when dealing with uniaxial incommensurate phases, one should choose the direction of incommensuration *along* the strip, to avoid imposing some (commensurate) wavelength by the boundary condition. For an infinite strip of width N , the correlation length $\xi(J, H/J, N)$ is calculated by

$$\xi^{-1} = \ln(\lambda_0/|\lambda_1|). \quad (4.1)$$

For the case of a single relevant (temperaturelike) variable t and one irrelevant variable u , finite-size scaling predicts (assuming isotropic scaling)

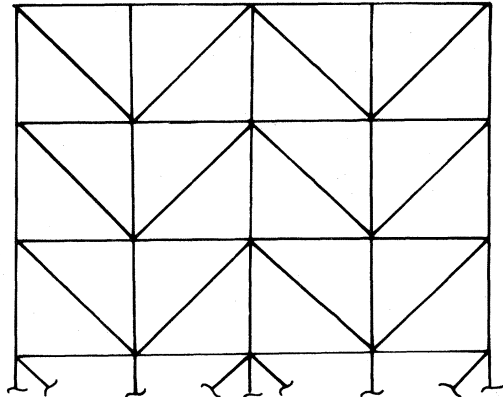


FIG. 4. Lattice used in numerical studies. For the transfer-matrix method, periodic boundary conditions (in the x direction) were used for an infinite strip. Monte Carlo simulations were done on square systems, with doubly periodic boundary conditions.

$$\xi(t, u, N) \simeq \frac{N}{N'} \xi \left[t \left(\frac{N}{N'} \right)^{y_t}, u \left(\frac{N}{N'} \right)^{y_u}, N' \right], \quad (4.2)$$

with $y_t > 0$ and $y_u < 0$.

Thus near criticality, the correlation length (along the direction of the strip) as calculated for a strip of width N , is related to that of a strip of width $N' < N$. Neglecting corrections due to the irrelevant operators³⁸ one obtains at criticality ($t=0$),

$$\frac{1}{N} \xi(0, N) = \frac{1}{N'} \xi(0, N'). \quad (4.3)$$

Therefore, the (scale-invariant) critical point is determined, for the case of our model, by solving (numerically) the equation

$$R_N(J_c) = \frac{\xi(J_c, N)/N}{\xi(J_c, N+2)/(N+2)} = 1. \quad (4.4)$$

That is, for any fixed value of H/J , Eq. (4.4) is solved for J_c . For temperatures T (equal to J^{-1}) $> J_c^{-1}$ the correlation length is finite, and $\xi(T, N) \sim \text{const}$ (independent to leading order of N), for $T \gg J_c^{-1}$. At criticality, $\xi(T_c, N) \sim N$. For $T < T_c$, in a phase with long-range order, $\xi(T, N) \sim \exp(aN)$, and thus we must have for $R_N(T)$

$$R_N(T) \sim \begin{cases} (N+2)/N, & T \rightarrow \infty \\ 1, & T = T_c \\ e^{-2a} < 1, & T < T_c. \end{cases} \quad (4.5)$$

For a model with a massless phase, one expects $R_N(T) \sim 1$ over a finite range of temperatures.

Critical exponents are determined from

$$\frac{1}{\nu} = y_t = \ln \left[\frac{\partial[\xi(J, N)/N]/\partial J}{\partial[\xi(J, N+2)/(N+2)]/\partial J} \right] / \ln \left[\frac{N}{N+2} \right]. \quad (4.6)$$

Again, for all fixed values of H/J one calculates y_t .

The spin-spin correlation function, as a function of distance l along the infinite strip direction, is given, for large distances, by

$$\langle S_0 S_l \rangle \sim (\lambda_1/\lambda_0)^l, \quad (4.7)$$

where λ_0 is the largest and λ_1 the next eigenvalue of the transfer matrix. However, if the second and third eigenvalues are a complex-conjugate pair, i.e., $\lambda_1 = |\lambda_1| e^{i\psi}$, the correlation function has the form

$$\langle S_0 S_l \rangle \sim (|\lambda_1|/\lambda_0)^l \cos(l\psi). \quad (4.8)$$

Thus the phase of λ_1 determines the wave vector associated with the dominant fluctuations (in the disordered phase) and that characteristic of the ordered phase (of the infinite system).

Equations (4.4) and (4.6) can be used to determine $T_c = J_c^{-1}$ and y_t only if the system scales isotropically. The correlation length measured is ξ_{\perp} in the direction along the strip; one investigates the manner in which ξ_{\perp} scales with the strip width N_{\parallel} . In some cases (for example, directed percolation,³⁹ Lifshitz point,¹⁸ and com-

mensurate-incommensurate transitions²⁷) scaling is anisotropic, and the more general form, as given by the relations

$$\xi_{\perp}(t, N_{\parallel}, N_{\perp}) = b^x \xi_{\perp}(b^y t, N_{\parallel}/b, N_{\perp}/b^x), \quad (4.9)$$

$$\xi_{\parallel}(t, N_{\parallel}, N_{\perp}) = b \xi_{\parallel}(b^y t, N_{\parallel}/b, N_{\perp}/b^x),$$

holds. Taking the limit $N_{\parallel}, N_{\perp} \rightarrow \infty$, t finite, one obtains

$$\xi_{\perp}(t, \infty, \infty) \simeq t^{-x/y} \xi_{\perp}(1, \infty, \infty),$$

$$\xi_{\parallel}(t, \infty, \infty) \simeq t^{-1/y} \xi_{\parallel}(1, \infty, \infty),$$

therefore identifying $\nu_{\parallel} = 1/y$ and $\nu_{\perp} = x/y$. Thus for an infinite strip, $N_{\perp} \rightarrow \infty$ and N_{\parallel} finite, one has

$$\xi_{\perp}(t, N_{\parallel}) = b^{\nu_{\perp}/\nu_{\parallel}} \xi_{\perp}(t b^{1/\nu_{\parallel}}, N_{\parallel}/b).$$

For isotropic scaling $\nu_{\perp}/\nu_{\parallel} = 1$, and one obtains the form (4.2).

A most useful function to calculate,⁴⁰ in order to check whether the scaling behavior is isotropic, is ($T = J^{-1}$)

$$Y_N = \ln \frac{\xi_{\perp}(T, N)}{\xi_{\perp}(T, N-2)} / \ln \frac{N}{N-2}. \quad (4.10)$$

In the asymptotic ($N \rightarrow \infty$) regime, one expects this function to behave as⁷

$$Y_N \sim \begin{cases} e^{-\alpha N}, & T > T_c \\ \nu_{\perp}/\nu_{\parallel}, & T = T_c \\ N, & T < T_c. \end{cases} \quad (4.11)$$

Therefore, for $N \rightarrow \infty$ one expects

$$Y_N \sim \begin{cases} 0, & T < T_c \\ \nu_{\perp}/\nu_{\parallel}, & T = T_c \\ \infty, & T < T_c. \end{cases} \quad (4.12)$$

If the approach to the asymptotic region is not too slow, i.e., $Y_N(T)$ does behave in the predicted manner, one may identify T_c by solving numerically the equation

$$Y_N(T_c) = Y_{N'}(T_c) = [\nu/\nu']_{N, N'}, \quad (4.13)$$

where $[\nu_{\perp}/\nu_{\parallel}]_{N, N'}$ is the estimate of the ratio $\nu_{\perp}/\nu_{\parallel}$ as based on strips of width N, N' .

We turn now to describe our results for the ATNNI model. The quantity $R_N(T)$ was calculated for $N=4, 6$, and 8 (the widest strip we used had $N=10$ independent sites—which necessitates finding the largest eigenvalue of a $2^{11} \times 2^{11}$ matrix). This was done for a sequence of fixed values of H/J . For $0 \leq H/J \leq 2.3$, we found $R_N(T)$ to vary monotonously with T (see Fig. 5), crossing the value $R_N(T_c) = 1$ at a set of points $T_c(H/J)$. The resulting values as obtained from the widest strips are shown in Fig. 2. It is important to note the monotonous variation, even close to the degeneracy point. However, for $H/J > 2.4$, this situation changes. For $H/J = 2.6$ and 2.8, we found that $R_N(T)$ is markedly nonmonotonic; it has loops that persist for the largest sizes studied. As H/J increases, these loops become much smaller and disappear. We interpret these loops as the manner in which the finite system approaches the behavior expected when the infinite

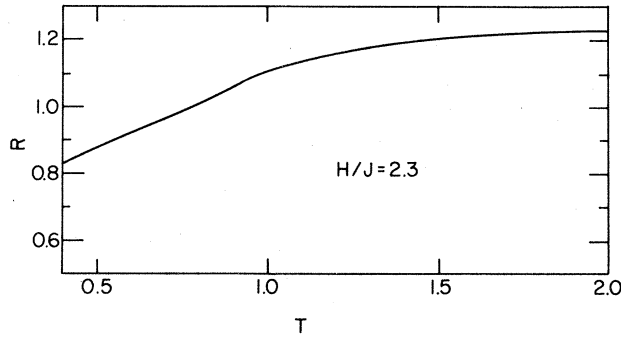


FIG. 5. Ratio $R(J^{-1})$, Eq. (4.4) for strips of widths 8, 10. For $H/J \leq 2.3$ monotonic behavior was found.

system has a massless phase over a finite range of temperatures, i.e., $R_N(T) \simeq 1$ for a range of temperatures. These loops are pronounced in the regime $2.4 < H/J \leq 3.0$; thus this is the range of H/J values in which we suspect to find the intermediate floating phase discussed in Secs. II and III. For higher H/J values our results indicate a direct transition from the disordered to the commensurate phase. A sequence of $R(T)$ curves is shown in Fig. 6(b). This figure also shows the variation of the wave vector, as determined from the phase of the second-largest eigenvalue. For $H/J < 2.4$, we find $\psi = 0$ for temperatures near the transition line. As T increases, the real second eigenvalue splits into a complex-conjugate pair at some $T_N^D(H/J)$. For $N = 10$, and fixed $T = 1.6$, we

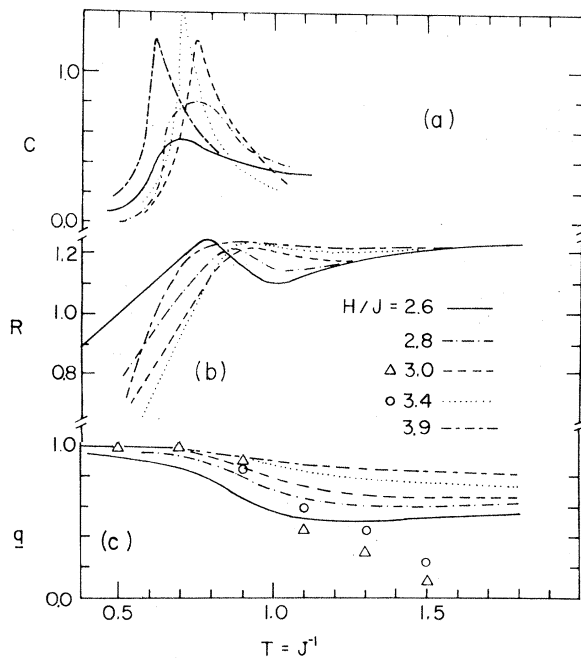


FIG. 6. (a) Specific-heat data from Monte Carlo ($N = 18$) for various H/J values. Note the sharpness of peaks for $H/J > 3.0$. (b) Ratio $R(J^{-1})$ of Eq. (4.4), using strips of 8, 10. Note the nonmonotonic behavior for $H/J = 2.6$ and 2.8. (c) Variation of the phase q (see text), from the transfer matrix (\circ) and from Monte Carlo (Δ). The Monte Carlo data are for 18×18 systems; still significant size dependence is found.

found the value of H/J at which this occurs to be within 0.5% of the value (~ 1.90) obtained by Verhagen.³¹

For $H/J > 2.4$, we find $\psi \neq 0$; in Fig. 6(c) we plot $q = \psi/(2\pi/3)$ as a function of T for various fixed H/J . Again, the situation is markedly different for $2.4 < H/J \leq 3.0$ and $H/J > 3.0$. In the former regime, q shows relatively fast variation in the region where loops of $R_N(T)$ are found, and at T_c [determined from $R_N(T_c) = 1$] we find $q < 1$ ($q = 1$ characterizes the commensurate phase). For $H/J > 3.0$, q varies slowly, slightly overshooting and approaching the commensurate value from above as $T \rightarrow T_c(H/J)$. These results indicate that the massless phase is characterized by an incommensurate wave vector, whereas in the regime of a single direct transition to the commensurate phase, $q = 1$ at T_c (and stays locked for $T < T_c$).

The difference between the regime $2.4 < H/J \leq 3.0$ and other H/J values is dramatically seen in the behavior of the functions $Y_N(T)$. In Figs. 7 and 8 we show this function evaluated for sizes $N = 4, 6$, and 8. In the regions where no massless phase is expected, Y_N behaves precisely as expected from Eq. (4.11) and the discussion that follows them. That is, for $H/J = 3.9, 3.4, 2.1$, and 0.2, the function has very small values at high temperatures; it increases dramatically as T decreases. The values of $\nu_{\perp}/\nu_{\parallel}$ (as determined from crossing of pairs of Y_N/Y_{N-2} curves) are close to 1, indicating isotropic scaling, although it is clearly seen that the approach to $\nu_{\perp}/\nu_{\parallel} = 1$ with size is not monotonous. The function Y_N behaves very differently for $H/J = 2.6$ (Fig. 7). Here we see a large loop, which we interpret in the following manner. If the model exhibits a massless phase for $T_{PT} < T < T_{KT}$, one should find, for $N \rightarrow \infty$,

$$Y_{\infty} \simeq \begin{cases} 0, & T_{KT} < T \\ 1, & T_{PT} < T < T_{KT} \\ \frac{1}{2}, & T = T_{PT} \\ \infty, & T < T_{PT} \end{cases} \quad (4.14)$$

The value $\nu_{\perp}/\nu_{\parallel} = \frac{1}{2}$ at the Pokrovsky-Talapov²⁶ (PT) transition was found by Schulz.²⁷ Clearly, the function $Y_N(T)$ as shown in Fig. 7 is consistent⁴¹ with the manner in which Y_N (for N finite) would approximate Y_{∞} that has the form (4.14).

All these findings are consistent with the phase diagram of Fig. 2. For $H/J < 2.4$, we find a single transition, to the 2×1 phase. For $2.4 < H/J \leq 3.0$, the disordered and commensurate phases are separated by an intermediate floating (massless) phase. This phase is bounded at high temperatures by a Kosterlitz-Thouless (KT) transition, whereas at low temperatures by a commensurate-incommensurate transition. At $H/J \approx 3.0$ we find a Lifshitz point; for $3.0 < H/J < 4.8$ the system undergoes a single, direct transition to the commensurate phase.

In order to determine the universality class of the single transitions we calculated y_T as a function of H/J using Eq. (4.6). The results, for various strip widths are shown on Fig. 9. For $H/J < 2.4$ the transition is Ising type; one should, however, note the relatively slow convergence with

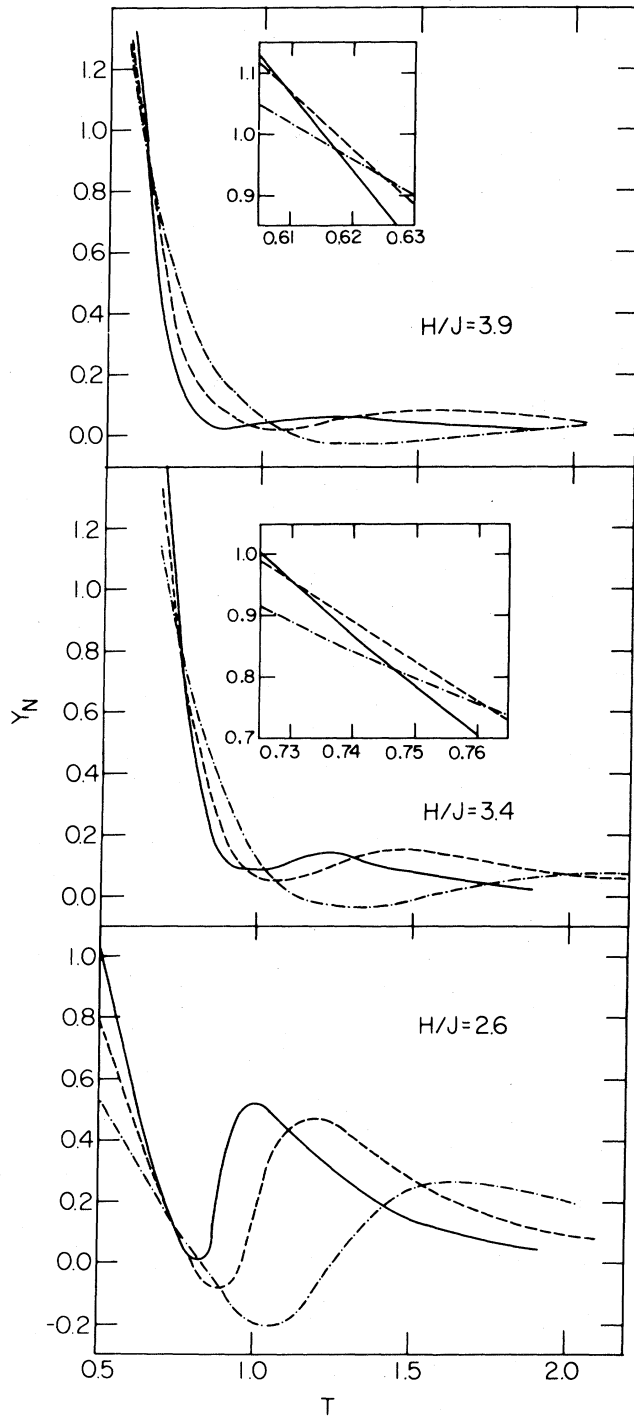


FIG. 7. The function Y_N , Eq. (4.10), for a set of H/J values, $N=10$ (solid line), 8 (dashed), and 6 (dotted-dashed). While the curves for $H/J=3.9$ and 3.4 behave according to Eq. (4.11), that of $H/J=2.6$ seems to approximate (4.14), that of $H/J=2.6$ seems to approximate (4.14). For 3.9 and 3.4 , the intersection point yields T_c in accord with (4.4), and with isotropic scaling.

size and large variation with H/J . Both these effects are due to the influence of irrelevant operators, and the fact that the temperaturelike (nonlinear) scaling field is a function of both J and H . Clearly, in order to reliably determine the critical exponents, calculations with wider strips,

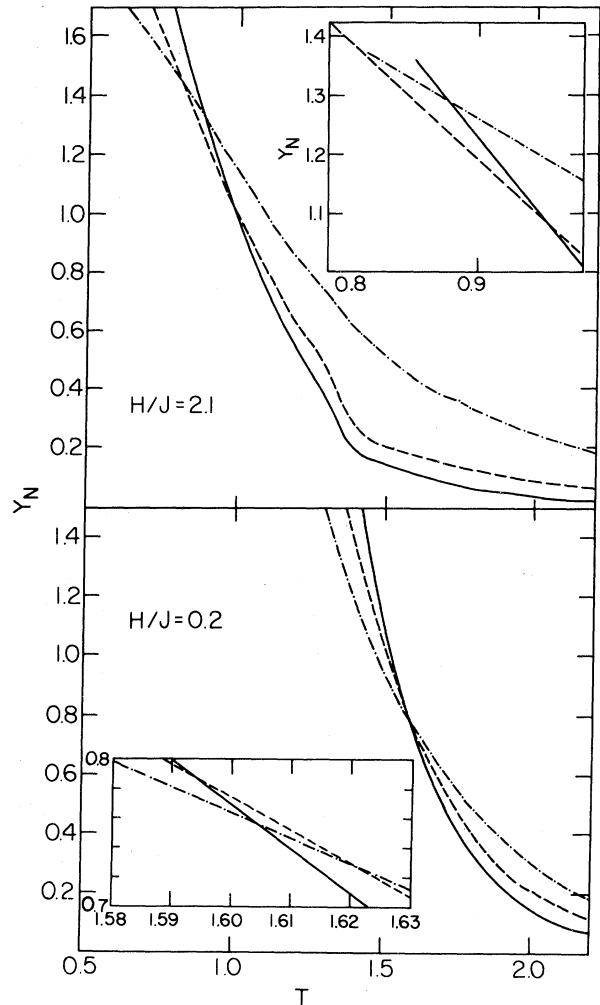


FIG. 8. The function Y_N , $N=10$ (solid lines), 8 (dashed), and 6 (dotted-dashed). For $H/J=0.2$ and 2.1 , the value of v_{\perp}/v_{\parallel} scales (slowly) towards 1; the function behaves as predicted by (4.11).

and methods such as recently proposed by Barber⁴² are needed. Here we tried to extract better estimates of the exponents by noting that corrections to scaling, due to irrelevant operators, should decrease when one scales at or

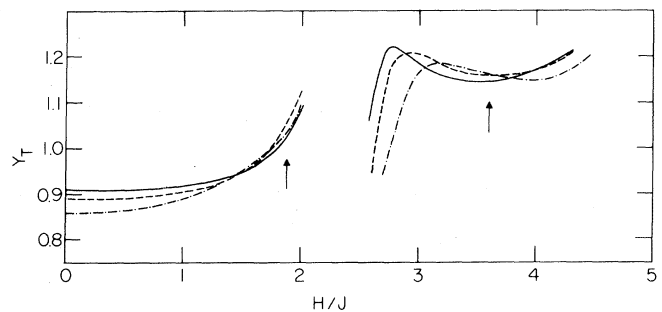


FIG. 9. Thermal exponent y_T , calculated for fixed values of H/J , using Eq. (4.6) with strips of widths 4, 6, 8, and 10 (respectively, dotted-dashed, dashed, and solid lines). Arrows indicate the fixed point [Eq. (4.15)]. For $H/J < 2.4$, $y_T=1$ (Ising) is expected. For $3 < H/J$ we find a single, CP transition.

near the fixed-point Hamiltonian, characterized by J^* and H^* . In order to identify the fixed point, we solved the equations⁴³ (requiring scaling for both J and H)

$$\begin{aligned} \frac{1}{N} \xi(J^*, H^*, N) &= \frac{1}{N+2} \xi(J^*, H^*, N+2) \\ &= \frac{1}{N+4} \xi(J^*, H^*, N+4) \end{aligned} \quad (4.15)$$

numerically, for J^* and H^* , with $N=6$.

For $H/J > 4.4$, we run into severe convergence problems; for $0 < H/J < 4.4$, Eqs. (4.15) have two solutions, at $(J^{-1}, H/J) = (1.14, 1.86)$ and $(J^{-1}, H/J) = (0.70, 3.58)$. The first of these solutions we interpret as the Ising fixed point, at which we obtained $y_T^{[8]} = 1.043$ and $y_T^{[10]} = 1.019$. The second fixed point characterizes the single direct transition from the disordered to the commensurate phase, and we find $y_T^{[8]} = 1.159$ and $y_T^{[10]} = 1.146$. These latter values are about 4% below the three-state Potts value⁴⁴ of 1.2; nevertheless, we do not feel this to be sufficient evidence to claim that this transition is characterized by exponents that are not three-state Potts type.

In summary, we have presented evidence, based on phenomenological renormalization-group techniques, that the phase diagram of the ATNNI model (2.1) is that of Fig. 2. However, we do feel that some aspects of this phase diagram need further substantiation. In particular, firmer checks on the existence and extent of the incommensurate phase, as well as for the distinctly different critical behavior for $2.4 < H/J \lesssim 3.0$ vs $H/J \gtrsim 3.0$, are needed. For this purpose we have performed Monte Carlo simulations of the ATNNI model.

V. MONTE CARLO SIMULATIONS

In order to present further evidence for the phase diagram of Fig. 2, we calculated several thermodynamic functions. The specific heat should exhibit a sharp peak in the regimes where single (Ising or CP) transitions are expected. In the incommensurate phase the situation is more involved; even though a divergence is expected as the commensurate phase is approached from above, the specific heat should have a broader, asymmetric peak. More significant is the scaling behavior of the (wave-vector-dependent) susceptibility. In the incommensurate phase the susceptibility, or Fourier transform of the spin-spin correlation function $\chi(q)$ should diverge for some incommensurate ($q \neq 1$) value of the wave vector. That is, for a sequence of finite systems, $\chi(q_{\max})$ should scale with size for $q_{\max} \neq 1$. In order to check these points, standard (Metropolis) Monte Carlo simulation was performed for $N \times N$ lattices schematically depicted in Fig. 4. When $N=6n$, this lattice allows for both ground states simultaneously, with doubly periodic boundary conditions. In the 2×1 phase [Fig. 1(c)] calculations were performed for 8×8 , 10×10 , 14×14 , 16×16 , 18×18 , and 20×20 lattices, whereas in the $\sqrt{3} \times \sqrt{3}$ phase [Fig. 1(d)] we considered 6×6 , 12×12 , 18×18 , and 24×24 lattices. For $H/J < (H/J)^*$, in the region of the 2×1 phase, the maximum of the specific heat C scales with size; $C_{\max} \sim \ln N$, indicating that the transition belongs to the Ising universality class. For $2.4 < H/J < 3.0$, $q(T)$ has a broader peak

for all lattice sizes. We observe, that for $2.4 < H/J < 2.8$, the specific-heat peaks are asymmetric with respect to the temperature around the maxima, which may reflect the absence of critical divergences on the commensurate side of the commensurate-incommensurate transition, as predicted by Schulz. But even carefully performed ($\sim 0.5 \times 10^5$ flips per spin) long simulations, annealing from high temperature, show only slight increase of C_{\max} with size. For $H/J = 2.6, 2.7, 2.8$, and 2.9 , such runs have been performed and C_{\max} -vs- $\ln N$ as well as $\ln C_{\max}$ -vs- $\ln N$ plots seem to indicate saturation. In Fig. 10 we show the specific-heat peaks for $H/J = 2.9$ for all lattice sizes. For $H/J > 3.0$, the specific heat shows a sharp peak which scales with increasing lattice size [see Figs. 2(a) and 10]; $\ln C_{\max} \sim w \ln N$ with a slope $w = 2\alpha/(2-\alpha)$ which varies with H/J . This variation corresponds to values of the specific-heat exponent $0.45 \lesssim \alpha \lesssim 0.55$. Such values are consistent with those found from simulations of small three-state Potts systems.⁴⁵ The locations of the specific-heat maxima are shown in the phase diagram of Fig. 2.

In the 2×1 phase the order parameter $M_{2 \times 1}$ fluctuates above T_c and increases rapidly below T_c to its maximum value. In the $\sqrt{3} \times \sqrt{3}$ phase, for $H/J > 3.0$, the appropriate order parameter $M_{\sqrt{3} \times \sqrt{3}}$ fluctuates strongly above T_c and tends to its ground-state value for temperatures $T_0 < T_c$. The susceptibilities, $\chi(q=0, T) = \chi_{2 \times 1}(T)$ and $\chi(q=1, T) = \chi_{\sqrt{3} \times \sqrt{3}}(T)$, associated with the corresponding order parameter were also calculated. Whereas for $H/J \geq 3.0$, $\chi_{\sqrt{3} \times \sqrt{3}}(T)$ always diverges, as the temperature approaches (from above) the value at which the specific heat is maximum, showing a clear scaling behavior, we find no such divergence for $H/J \lesssim 3.0$. Here $\chi_{\sqrt{3} \times \sqrt{3}}(T)$ is of the order of $\chi_{2 \times 1}(T)$. We also calculated $\chi(\vec{k})$, the susceptibility associated with wave vector $\vec{k} = (2\pi/a, 2\pi q/3b)$ at fixed $T = J^{-1}$ and H/J , mostly

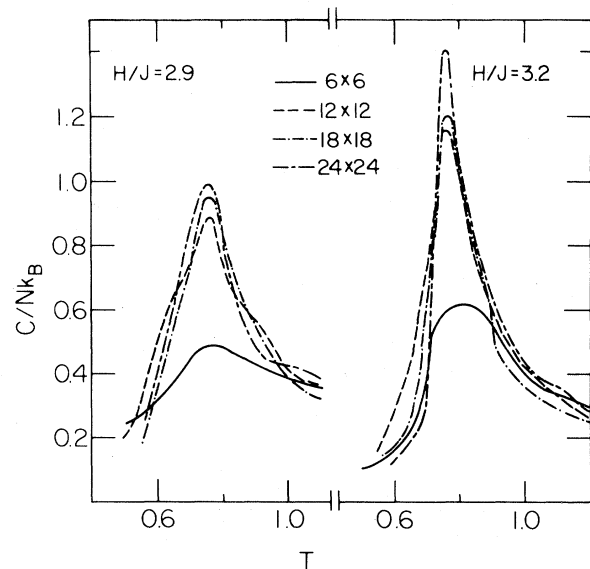


FIG. 10. Specific heat per spin for $H/J = 2.9$ and 3.2 . Note sharpness and increase of C_{\max} with size for $H/J = 3.2$. For $H/J \lesssim 2.9$ broader and more asymmetric peaks were found, with little apparent scaling with size.

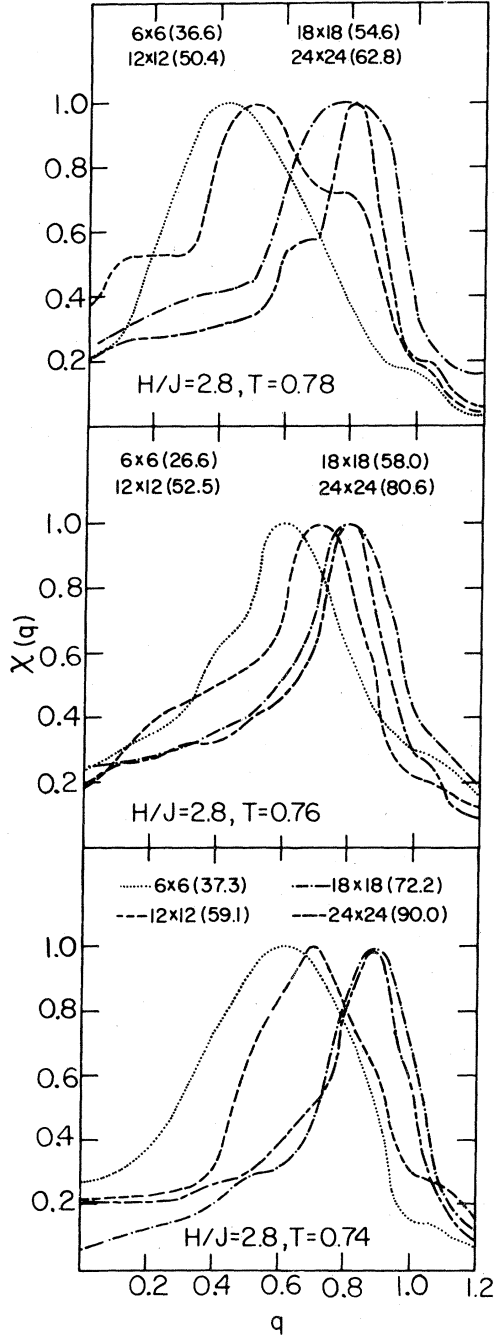


FIG. 11. Wave-vector-dependent susceptibility per spin, $\chi(q) = \sum_{\vec{R}} \langle S(0)S(R) \rangle \exp(i\vec{q} \cdot \vec{R})$. In parentheses, next to the lattice sizes, the maximum value (all curves are normalized to have the same maximal values). $q=1$ corresponds to the commensurate phase. For all three temperatures $q_{\max} < 1$.

in the disordered regime $T > T_c(H/J)$. Values of $q_{\max}(T, H/J)$ at which $\chi(q)$ is maximum were identified [see Figs. 2(c) and 11–13]. We find that for sufficiently large values of H/J , near the transition $q_{\max} = 1.0$, i.e., the transition is to a commensurate phase.

In order to get further information about the region of the massless phase we studied the scaling behavior of

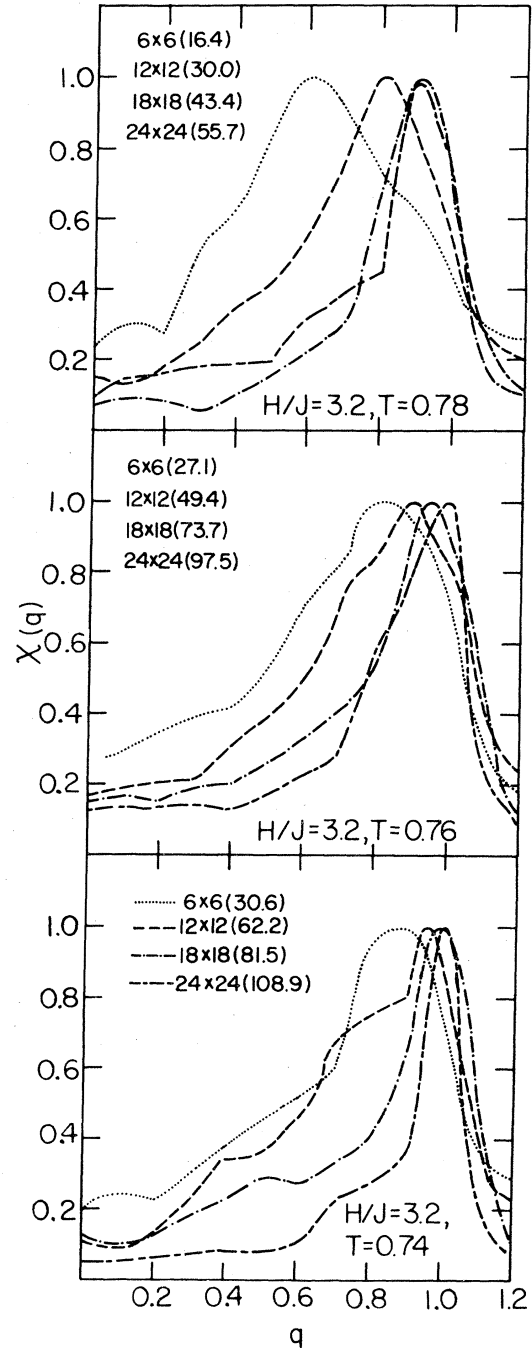


FIG. 12. Wave-vector-dependent susceptibility per spin, $\chi(q) = \sum_{\vec{R}} \langle S(0)S(R) \rangle \exp(i\vec{q} \cdot \vec{R})$. In parentheses, next to the lattice sizes, the maximum value (all curves are normalized to have some maximal values). $q=1$ corresponds to the commensurate phase. Note that as $T \rightarrow T_c^+$, $q_{\max} \rightarrow 1$.

$\chi(q_{\max})$ for $H/J=2.8, 3.2$, and 3.6 as a function of size. We performed long runs ($\sim 10^5$ flips per spin) annealing from high temperatures in the temperature region close to the specific-heat maxima for all lattice sizes. For $H/J=2.8$ we observe scaling behavior; $\ln\chi(q_{\max}) \sim \bar{w} \ln N$, for temperature $T \leq 0.78$. This is shown in Fig. 14. It is important to note that for all lattice sizes the

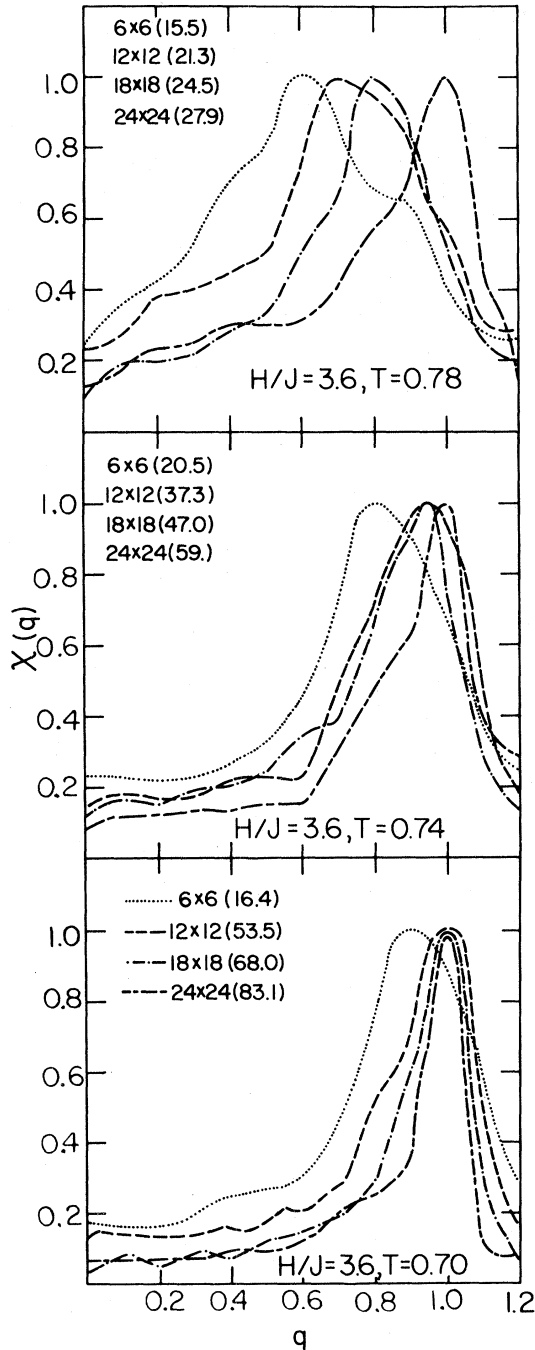


FIG. 13. Wave-vector-dependent susceptibility per spin, $\chi(q) = \sum_{\vec{R}} \langle S(0)S(R) \rangle \exp(i\vec{q} \cdot \vec{R})$. In parentheses, next to the lattice sizes, the maximum value (all curves are normalized to have some maximal values). $q=1$ corresponds to the commensurate phase. Note that as $T \rightarrow T_c^+$, $q_{\max} \rightarrow 1$.

values q_{\max} ($T, H/J=2.8$) are smaller than the commensurate value $q_{\max}=1.0$ (see Fig. 11). This has to be compared to the behavior at $H/J=3.2$. Here we also find scaling behavior of $\ln\chi(q_{\max})$ for $T \leq 0.78$, but for values of q_{\max} very close to the commensurate value; see Figs. 12 and 15. Finally, for $H/J=3.6$ we see (Fig. 16) scaling

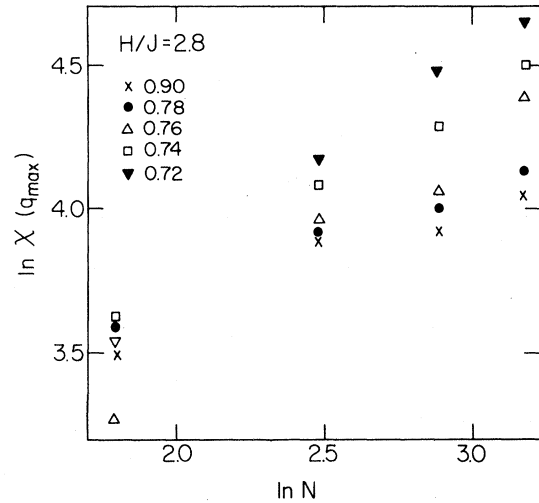


FIG. 14. Maximum value of χ vs size N . For $T \leq 0.76$, χ_{\max} scales with size, $\ln\chi(q_{\max}) \sim \ln N$, even though $q_{\max} < 1$ (see Fig. 11), indicating existence of a massless incommensurate phase.

behavior of $\ln\chi(q_{\max})$ for $T \leq 0.78$, but here the wave vector is already locked at $q_{\max}=1.0$ for the largest lattice size (Fig. 13). The scaling behavior of $\chi(q_{\max})$ at incommensurate wave vectors $q_{\max} < 1$ is added evidence for a narrow strip of incommensurate massless phase in the region $2.4 \leq H/J \leq 3.0$. The fact that for $H/J \geq 3.0$ scaling behavior is observed only for $q=1$ indicates that in this regime the transition is directly to the commensurate phase. Thus our simulations are completely consistent with the phase diagram of Fig. 2.

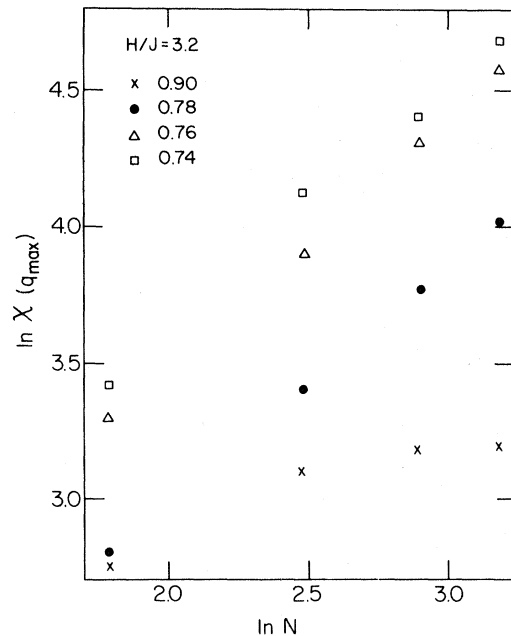


FIG. 15. $\ln\chi(q_{\max})$ vs $\ln N$, $H/J=3.2$. Scaling is seen for $T \leq 0.78$. For $T=0.78$, $q_{\max} < 1$ (but rather close); for $T=0.76$ and 0.74 , $q_{\max}=1$ (see Fig. 12).

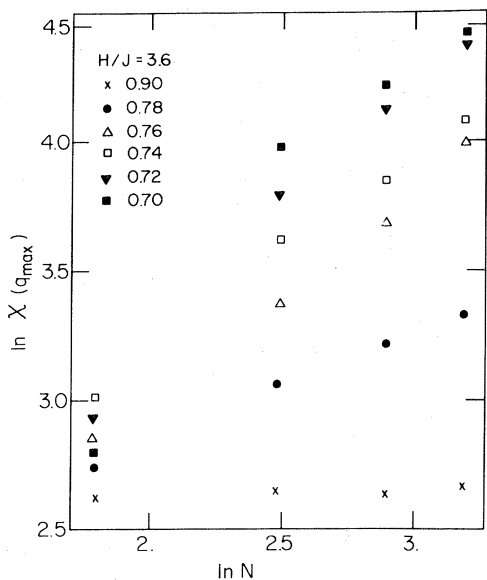


FIG. 16. $\ln \chi(q_{\max})$ vs $\ln N$, $H/J=3.6$. In the region where scaling is clearly observed, $q_{\max}=1$, indicating direct transition to the commensurate phase.

VI. SUMMARY AND DISCUSSION

We have studied the ATNNI model; an Ising model in an external field with nearest-neighbor antiferromagnetic interactions on an anisotropic triangular lattice. Physical realizations may include noble gases physisorbed on the (110) face of a bcc crystal, where the adsorption sites form a centered rectangular array.

The ATNNI model has simple interactions and local variables. Nevertheless, we found a complex and interest-

ing phase diagram, with two competing commensurate phases, an incommensurate phase with algebraic decay of correlations, a uniaxial commensurate-incommensurate transition, a Lifshitz point, and a single continuous transition (in the CP class) from the disordered to a commensurate state, for which the Lifshitz condition is not satisfied. The existence of such a transition is not allowed by mean-field theory, and it provides a further example to the central role played by fluctuations in critical behavior in two dimensions. The thermal exponent of this transition is very close to that of the three-state Potts model.

Our results are consistent with existing theories of the commensurate-incommensurate transition; however, further studies, based on wider strips, seem to be necessary in order to compare results quantitatively. Also, properties of the Lifshitz point should be investigated in more detail.

We believe that the ATNNI model can serve as a most convenient testing ground for both our theoretical understanding of many interesting phenomena in two dimensions as well as for various novel calculation techniques.

ACKNOWLEDGMENTS

Our work on the ATNNI model started as a joint project with W. Kinzel, who suggested the problem and taught us the phenomenological renormalization-group technique. We had most useful discussions with K. Binder, V. Emery, D. Derrida, R. Griffiths, D. Mukamel, M. P. M. den Nijs, P. Nightingale, I. Peschel, H. Schulz, and other participants of the Summer Institute on Statistical Mechanics, 1983, funded by the A. Einstein Center for Theoretical Physics at the Weizmann Institute. We acknowledge financial support from Minerva and the Heinemann Foundation (B.S.) and the Batsheva de Rothschild Foundation (E.D.).

- ¹R. J. Baxter, *J. Phys. A* **13**, L61 (1980); *J. Stat. Phys.* **26**, 427 (1981).
- ²D. A. Huse, *Phys. Rev. Lett.* **49**, 1121 (1982).
- ³R. J. Baxter and P. A. Pearce, *J. Phys. A* **16**, 2239 (1983).
- ⁴B. Nienhuis, *Phys. Rev. Lett.* **49**, 1062 (1982).
- ⁵J. V. José, L. P. Kadanoff, S. Kirkpatrick, and D. R. Nelson, *Phys. Rev. B* **16**, 1217 (1977); L. P. Kadanoff and A. C. Brown, *Ann. Phys. (N.Y.)* **121**, 318 (1979); H. J. F. Knops, *ibid.* **128**, 448 (1980); J. L. Black and V. J. Emery, *Phys. Rev. B* **23**, 429 (1981).
- ⁶R. H. Swendsen, in *Real Space Renormalization*, edited by T. W. Burkhardt and J. M. J. van Leeuwen (Springer, Berlin, 1982).
- ⁷P. Nightingale, *J. Appl. Phys.* **53**, 7927 (1982).
- ⁸For some recent reviews and conference proceedings, see O. E. Vilches, *Annu. Rev. Phys. Chem.* **31**, 463 (1980); in *Ordering in Two Dimensions*, edited by S. K. Sinha (North Holland, Amsterdam, 1980); *Surf. Sci.* **125**, 1 (1983).
- ⁹M. Jaubert, A. Glachant, M. Bienfait, and G. Boato, *Phys. Rev. Lett.* **46**, 1679 (1981); R. Imbihl, R. J. Behm, K. Christmann, G. Ertl, and T. Matsushima, *Surf. Sci.* **117**, 257 (1982); W. C. Marra, P. H. Fuoss, and P. E. Eisenberger, *Phys. Rev. Lett.* **49**, 1169 (1982).
- ¹⁰E. Domany, M. Schick, and J. S. Walker, *Phys. Rev. Lett.* **38**, 1148 (1977); E. Domany, M. Schick, J. S. Walker, and R. B. Griffiths, *Phys. Rev. B* **18**, 2209 (1978).
- ¹¹B. Schaub and E. Domany, *Phys. Rev. B* **28**, 2897 (1983).
- ¹²R. M. Hornreich, R. Liebmann, H. G. Schuster, and W. Selke, *Z. Phys. B* **35**, 91 (1979); W. Selke and M. E. Fisher, *ibid.* **40**, 71 (1980); P. Bak and J. van Boehm, *Phys. Rev. B* **21**, 5297 (1980).
- ¹³M. N. Barber and P. M. Duxbury, *J. Stat. Phys.* **29**, 427 (1982); W. Selke, *Z. Phys. B* **43**, 335 (1981).
- ¹⁴J. Villain and P. Bak, *J. Phys.* **42**, 657 (1981).
- ¹⁵S. Ostlund, *Phys. Rev. B* **24**, 398 (1981).
- ¹⁶W. Selke and J. M. Yeomans, *Z. Phys. B* **46**, 311 (1982).
- ¹⁷W. Kinzel, W. Selke, and K. Binder, *Surf. Sci.* **121**, 13 (1982); **125**, 74 (1983).
- ¹⁸R. M. Hornreich, M. Luban, and S. Shtrikman, *Phys. Rev. Lett.* **35**, 1678 (1975).
- ¹⁹D. A. Huse and M. E. Fisher, *Phys. Rev. Lett.* **49**, 793 (1982); and *Phys. Rev. B* **29**, 239 (1984); M. Kardar and A. N. Berker, *Phys. Rev. Lett.* **48**, 1552 (1982).
- ²⁰M. P. M. den Nijs (private communication).
- ²¹S. Goshen, D. Mukamel, and S. Shtrikman, *Int. J. Magn.* **6**, 221 (1974).

- ²²S. F. Howes, L. P. Kadanoff, and M. P. M. den Nijs, Nucl. Phys. B 215, 169 (1983).
- ²³S. F. Howes, Phys. Rev. B 27, 1762 (1983).
- ²⁴F. D. M. Haldane, P. Bak, and T. Bohr, Phys. Rev. B 28, 2743 (1983); H. J. Schulz, *ibid.* 28, 2746 (1983).
- ²⁵I. Tosatti, Solid State Commun. 25, 637 (1978).
- ²⁶V. L. Pokrovsky and A. L. Talapov, Phys. Rev. Lett. 42, 65 (1979).
- ²⁷H. J. Schulz, Phys. Rev. B 22, 5274 (1980).
- ²⁸J. Villain, in *Ordering in Strongly Fluctuating Condensed Matter Systems*, edited by T. Riste (Plenum, New York, 1980), p. 221; P. Bak, Rep. Prog. Phys. 45, 587 (1982).
- ²⁹M. E. Fisher and M. N. Barber, Phys. Rev. Lett. 28, 1516 (1972); M. E. Fisher, in *Proceedings of the International School of Physics, "Enrico Fermi," Varenna, 1970, Course No. 51*, edited by M. S. Green (Academic, New York, 1971).
- ³⁰R. M. F. Houtappel, Physica 16, 425 (1950).
- ³¹A. M. W. Verhagen, J. Stat. Phys. 15, 219 (1976) (we thank I. Peschel for bringing this paper to our attention); P. Rujan, *ibid.* 29, 231 (1982); 29, 247 (1982); and (unpublished).
- ³²K. Y. Lin and F. Y. Wu, Z. Phys. B 33, 181 (1979).
- ³³J. Muller-Hartmann and J. Zittartz, Z. Phys. B 27, 261 (1977).
- ³⁴J. Doczi-Reger and P. C. Hemmer, Physica 108A, 531 (1981).
- ³⁵W. Kinzel and M. Schick, Phys. Rev. B 23, 3435 (1981).
- ³⁶S. Alexander, Phys. Lett. 54A, 353 (1975).
- ³⁷S. N. Coppersmith, D. S. Fisher, B. I. Halperin, P. A. Lee, and W. F. Brinkman, Phys. Rev. B 25, 349 (1982).
- ³⁸V. Privman and M. E. Fisher, J. Phys. A 16, L295 (1983).
- ³⁹W. Kinzel and J. Yeomans, J. Phys. A 14, L163 (1981).
- ⁴⁰We thank W. Kinzel for pointing this out.
- ⁴¹This is to be compared with a recent study of the H/Fe model, by Kinzel, Phys. Rev. Lett. 14, 996 (1983). He finds loops such as we find for $H/J=2.6$; however, the curves for various sizes cross only at high temperatures. We also see crossing at such points, but believe that with increasing size they should move to $T \rightarrow \infty$, whereas the curves should approach one another in the loop regions.
- ⁴²M. N. Barber, Phys. Rev. B 27, 5879 (1983).
- ⁴³This was suggested by P. Nightingale.
- ⁴⁴M. P. M. den Nijs, J. Phys. A 12, 1857 (1979).
- ⁴⁵K. Binder, J. Stat. Phys. 24, 69 (1981).